DOI: 10.51984/3FV3GG10

وقائع مؤتمرات جامعة سبها
Sebha University Conference Proceedings
Confrence Proceeeding homepage: http://www.sebhau.edu.ly/journal/CAS

Numerical Investigation of a PEC-Backed PVDF/MWCNT/Fe_3O_4 Nanocomposite Microwave Absorber in the X–Ku Band Using HFSS Floquet-Port Simulation

Majdi Khalfalla [a*], Marai Abousetta [b]

[a] Renewable Energy Department, Natural Resources Engineering College, Bir-Alghanam, University of Zawia, Libya
[b] Electrical and Computer Engineering Department, School of Applied Sciences and Engineering, Libyan Academy for Postgraduate Studies - Tripoli, Libya

Keywords:
microwave absorber
PVDF
MWCNT
Fe_3O_4
reflection loss
HFSS
Floquet port
X-Ku band
impedance matching

ABSTRACT

Growing electromagnetic interference (EMI) and radar-signature concerns in the X and Ku microwave bands (8-18 GHz) have renewed interest in thin, lightweight, absorption-dominated composite materials as an alternative to bulky metallic shields. This work presents a numerical design study of a PVDF/MWCNT/Fe3O4 nanocomposite absorber backed by a perfect electric conductor (PEC) plane. A dispersive material model was built from representative low-frequency electromagnetic data combined with a Fe3O4-driven magnetic resonance placed at 14.5 GHz, and reflection loss was computed using the transmission-line model (TMM), the exact analytical solution for a homogeneous slab at normal incidence. A thickness sweep from 1.0 to 2.5 mm revealed a sharp, narrow band resonance instead of a gradual thickness-dependent trend. The best configuration, at 1.61 mm, reached a minimum reflection loss of -58.6 dB at 11.34 GHz, well beyond the -20 dB (99% absorption) target and deeper than comparable double and triple filler absorbers reported in the literature at similar thicknesses. The resonance arises from quarter-wavelength geometric matching coinciding with a loss tangent already elevated on approach to the assumed magnetic resonance, and it proved highly sensitive to thickness, with minimum reflection loss (RL_{min}) varying by over 30 dB across a 0.4 mm window, a finding with direct implications for manufacturing tolerance. These results were cross checked against an initial HFSS Floquet-port simulation, which was found to require a finer mesh before it can serve as independent verification this remains ongoing work, alongside experimental validation of the electromagnetic input data above 12 GHz.

دراسة عددية لممتص الموجات الدقيقة النانوي PVDF/MWCNT/Fe_3O_4 المدعوم بـ PEC في نطاق X–Ku باستخدام محاكاة HFSS Floquet-Port

مجدي خلف الله [a*] مرعي أبوستة [b]

[a] قسم الطاقة المتجددة، كلية هندسة الموارد الطبيعية بئر الغنم، جامعة الزاوية، ليبيا
[b] قسم الهندسة الكهربائية وهندسة الحاسوب، مدرسة العلوم التطبيقية والهندسة، الأكاديمية الليبية للدراسات العليا - طرابلس، ليبيا

الكلمات المفتاحية:
أنابيب الكربون النانوية متعددة الجدران
Fe_3O_4
فقدان الانعكاس
مادة ماصة للموجات الدقيقة

الملخص

أدى تزايد التداخل الكهرومغناطيسي (EMI) والقلق المتعلق بالبصمة الرادارية في نطاقي الموجات الدقيقة X وKu (نطاق 8-18 جيجاهرتز) إلى تزايد الاهتمام بالمواد المركبة الخفيفة الرقيقة ذات الامتصاص الغالب كبديل للدروع المعدنية الثقيلة. يقدم هذا العمل دراسة تصميم عددية لممتص من متراكب نانوي هجين PVDF/MWCNT/Fe3O4 مدعوم بسطح موصل كهربائي مثالي (PEC). تم بناء نموذج مادي مُشتت اعتماداً على بيانات كهرومغناطيسية تمثيلية عند الترددات المنخفضة، مضافاً إليها خاصية رنين مغناطيسي ناتجة عن Fe3O4

*Corresponding author:
E-mail addresses: majdi.khalfalla@zu.edu.ly ,(M. Abousetta) m.abousetta@academy.edu.ly
Article History : Received 30 May 2026 - Received in revised form 30 September 2026 - Accepted 11 November 2026

عند 14.5 جيجاهرتز، مع تطبيق إثارة بواسطة منفذ فلويك (Floquet-port) وسقوط عمودي للموجات، وتم حساب فقد الانعكاس باستخدام نموذج خط النقل (TMM)، وهو الحل التحليلي المضبوط لشريحة متجانسة تحت سقوط عمودي. أظهر كشف مسح السماكة من 1.0 إلى 2.5 مم عن رنين حاد وضيق النطاق بدل الاتجاه التدريجي المتوقع، وحقق أفضل تكوين، عند سماكة 1.61 مم، أقل قيمة لفقد الانعكاس بلغت 58.6- ديسيبل عند تردد 11.34 جيجاهرتز، متجاوزاً بذلك هدف 20- ديسيبل (امتصاص 99%) بفارق كبير، ومتفوقاً على ممتصات مشابهة ذات طبقتين أو ثلاث حشوات ورد ذكرها في الأدبيات عند سماكات مقاربة. ينشأ هذا الرنين من تطابق المعاوقة (Impedance-matching) الهندسي بطول ربع الموجة الذي يتزامن مع ارتفاع نسبة الفقد اقتراباً من الرنين المغناطيسي المفترض، وقد أظهر حساسية عالية للسماكة، إذ تراوحت قيمة أقل فقد انعكاس بأكثر من 30 ديسيبل ضمن نافذة سماكة مقدارها 0.4 مم فقط، وهي نتيجة لها انعكاسات مباشرة على هامش التفاوت المسموح بالتصنيع. وقد جرت مقارنة هذه النتائج بمحاكاة أولية عبر منفذ فلويك (Floquet-port) في HFSS، وتبين أنها تحتاج شبكة حسابية أدق لتكون تحققاً مستقلاً موثوقاً، وهذا عمل ما زال جارياً، إلى جانب التحقق التجريبي من البيانات الكهرومغناطيسية المُدخلة فوق 12 جيجاهرتز.

مطابقة المعاوقة
منفذ فلوكي
نطاق *X-Ku*
HFSS
PVDF.

1. Introduction

Electromagnetic interference (EMI) and unwanted radar reflections have become a significant concern due to the rapid growth and widespread use of radar, satellite, and dense wireless communication systems operating across the X-band and Ku bands (8 - 18 GHz). These difficult problems are unmanageable in aerospace and defense structures. Traditional methods, such as metallic shields, work almost entirely by reflection, which is effective for isolating a system from external EMI but has limited effect in reducing radar's structure signature, and they simply relocate the reflected energy elsewhere. Such methods are undesirable for applications where the main goal is to absorb the incident wave rather than redirecting it. Accordingly, conductive polymer nanocomposites loaded with dielectric and magnetic fillers have emerged. Moreover, these polymer nanocomposites are light in weight, have a tunable electromagnetic response, and are simple to process [1], [2]. EMI shielding performance is conventionally reported through shielding effectiveness (SE), decomposed into reflection and absorption contributions.

$$SE_T(dB) = SE_R + SE_A = 10log_{10}(P_T/P_I) \qquad (1)$$

where both PI and PT are incident and transmitted powers. Dubey et al. used this two-port formulation to show numerically that a CNT-loaded polypyrrole composite reaches a percolation threshold at as little as 2 wt% CNT loading, beyond which Shielding Effectiveness (SE) continues to rise only moderately, and that the resulting composite is absorption-dominated (SE_A ≫ SE_R) across the X-band [1]. Mohan et al. experimentally characterized a carbon-based epoxy nanocomposite shield across both the X- and Ku-bands using the same framework, confirming that broadband EMI performance is achievable with a single carbon-filler system when loading and thickness are tuned appropriately [2].

The present study targets configuration of single-port, PEC-backed radar absorbing material (RAM), for which the relevant measure is reflection loss (RL) rather than SE; the two metrics are related in spirit but not numerically interchangeable, and Section 2.2 defines the RL formula that is used in this work. In pure dielectric (carbon-only) absorbers are likely to reflect a large fraction of incident power is likely to be reflected at the front interface because their intrinsic impedance is poorly matched to free space. Magnetic fillers such as Fe_3O_4 (magnetite) are commonly used along with carbon nanofillers specifically to correct this impedance mismatch. The Fe_3O_4 contributes magnetic loss through natural resonance mechanisms that lead to raise the effective permeability of the composite, bringing its wave impedance closer to that of free space and thereby reducing the fraction of incident energy that is reflected before it can be absorbed [3], [4].

Shen et al. demonstrated this synergy clearly in a magnetic hollow mesoporous carbon system, where deliberate impedance matching was the design lever used to achieve strong broadband absorption [3], while Huang et al. showed that rod-shaped Fe_2O_3/Fe_3O_4/MWCNT composites benefit from the combined dielectric-magnetic loss mechanism. PVDF (polyvinylidene fluoride) has become a popular host matrix for this type of hybrid absorber because of its intrinsically higher dielectric permittivity relative to common epoxy hosts, its mechanical flexibility, and its compatibility with solution-casting or electrospinning fabrication routes. Adebayo et al. fabricated a Fe_3O_4/PVDF nanocomposite and by using finite-element simulation of the measured electromagnetic parameters, they reported a minimum reflection loss of −62.7 dB at 16.9 GHz for a 3.5 mm sample, attributing the result to favorable impedance matching arising from balanced dielectric and magnetic loss [5]. Yang et al. combined MWCNTs and Fe_3O_4 in a flexible silicone-rubber foam and likewise found that the magnetic filler shifted the dominant shielding mechanism toward absorption [6], and Li et al. showed for a PVDF-co-HFP/Fe_3O_4/reduced-graphene-oxide system that the strongest absorption band concurred with the classical quarter-wavelength interference matching condition rather than with the intrinsic loss peak alone [7]. Hollow or core–shell Fe_3O_4 morphologies have also been explored specifically to shift the magnetic resonance frequency upward into the Ku-band, since bulk Fe_3O_4 alone resonates well below 5 GHz [8]. outperform either filler type alone [4].

The second closely related design is absorber thickness. Because reflection loss is controlled by both the intrinsic loss tangent of the material and by constructive interference between waves reflected at the front face and at the PEC backing, the frequency at which RL is minimized shifts with thickness even for a fixed material composition. Ibrahim et al. demonstrated this trade-off directly using double-layer carbon-black/ferrite composites, tuning layer thickness to change the absorption minimum within the X-band [8][9]. For Fe_3O_4/MWCNT systems, Yuan et al. reported that coupling Fe_3O_4 nanocrystals to MWCNTs blue shifts the magnetic resonance frequency to around 9.1 GHz, substantially higher than the sub-5 GHz resonance of conventional bulk Fe_3O_4, which is what makes Fe_3O_4/carbon hybrids feasible absorbers in the higher-frequency Ku-band at all [10]. Yin et al. observed a related effect in anisotropic Fe_3O_4/graphene composites and found an optimal reflection loss of about −38.1 dB at 14.8 GHz for a 1.7 mm sample, showing that with the right filler morphology the magnetic loss peak can be placed usefully inside the Ku-band [11]. Based on this body of work, the present study investigates a PVDF matrix loaded with 5 wt% MWCNT and 20 wt% Fe_3O_4, aiming for RL below −20 dB across the frequency range of 8 to 18 GHz with a thickness not exceeding 2.5 mm, a constraint set by typical conformal-coating and weight-budget requirements. Rather than fabricate the composite experimentally, we carry out a purely numerical design study in Ansys HFSS, using a Floquet-port periodic unit cell to evaluate reflection loss directly from the simulated S11 parameter, and use a parametric sweep over range thickness to map the achievable design space before committing to a specific fabrication route.

2. Simulation Methodology

The overall simulation steps, starting from PUC geometry and boundary definition through the adaptive mesh-refinement loop to final RL extraction, is summarized in Figure1.

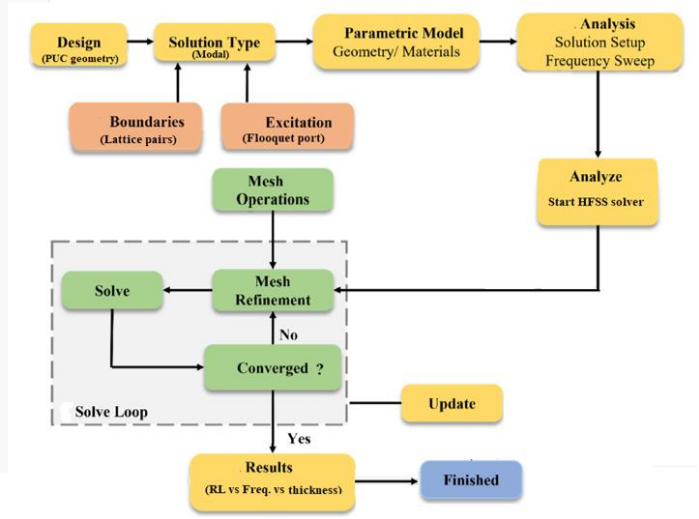


Fig. 1. Hierarchy of simulation steps followed in Ansys HFSS of study.

2.1 Absorber geometry and boundary conditions

The absorber was designed as a three-layer stack inside a rectangular periodic unit cell of 10 × 10 mm2 cross-sections, as shown in Figure. 2. From bottom to top, the stack consists of a 0.5 mm perfect electric conductor (PEC) backing plane, which represents a metallic substrate typical of an aerospace panel; the PVDF/MWCNT/Fe_3O_4 absorbing slab, whose thickness t was varied from 1.0 to 2.5 mm; and an air region of 6–7 mm extending up to a Floquet excitation port. Periodic (lattice-pair) boundary conditions were applied to the four side walls of the unit cell to emulate an infinite periodic array under normal-incidence plane-wave illumination, and the Floquet port was excited in the fundamental TE mode only consistent with normal incidence. The unit-cell period was kept below λ across the band, though the margin narrows at the upper edge.[12]

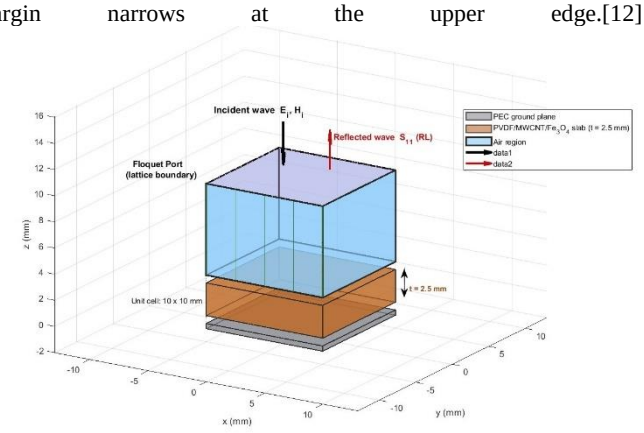


Fig. 2. Exported HFSS geometry of the periodic unit cell: PEC backing plane, PVDF/MWCNT/Fe_3O_4 absorbing slab, and the air region terminated by the Floquet port.

2.2 Dispersive material model

Reflection loss is highly sensitive to the frequency dependence of the complex relative permittivity (ε′, ε″) and permeability (μ′, μ″) of the absorbing layer, so a non-dispersive (single-frequency) material assignment has been considered inadequate for a design study spanning a full decade-and-a-half octave of bandwidth. Representative electromagnetic parameters consistent with reported values for MWCNT/Fe_3O_4 loaded polymer composites in the lower X-band [4], [6] were adopted as an anchor, and the dielectric response was extended toward 18 GHz using a decaying-exponential trend for ε′ and a saturating trend for ε″, reflecting the well-documented behavior of MWCNT conduction/interfacial-polarization loss networks approaching a high-frequency plateau [1], [4].

For the magnetic response, instead of assuming a flat non-dispersive permeability, a Lorentzian resonance feature was introduced with resonance frequency f_0 = 14.5 GHz and damping factor Δ, with static permeability μ_s = 2.3:

$$\mu'(f) = 1 + (\mu_s - 1)(f_0^2 - f^2)/[(f_0^2 - f^2)^2 + (f\Delta)^2] \quad (2)$$

$$\mu''(f) = (\mu_s - 1) \cdot f \cdot \Delta/[(f_0^2 - f^2)^2 + (f\Delta)^2] \quad (3)$$

This placement is directly motivated by the literature. Yuan et al. observed a superparamagnetic relaxation driven resonance at a frequency of 9.1 GHz in Fe_3O_4/MWCNT structures. This resonance was much higher in frequency compared to the resonance seen in pure Fe_3O_4, which occurs at less than 5GHz. They connected this shift in frequency to better absorption of signals in the Ku-band, which is why they think the improved absorption is happening.[10]Yin et al. separately reported optimal absorption at 14.8 GHz for an anisotropic Fe_3O_4/graphene composite of comparable thickness to the present design [11]. The 14.5 GHz value here sits between these two literature benchmarks and represents a physically motivated estimate for the Fe_3O_4-loaded PVDF/MWCNT system under study [13]. We emphasize that the range of 8–12 GHz of the input dispersion curve is treated as representative of measured composite behavior reported in the literature, while the 12.5–18 GHz band is a modeled extension using equations (2) and (3) and, in future work, should be validated against vector network analyzer characterization of the actual composite. The resulting ε′, ε″, μ′, and μ″ curves in Figure 3 were imported into HFSS as frequency-dependent datasets and linked to the slab material via piecewise-linear interpolation Table 1.

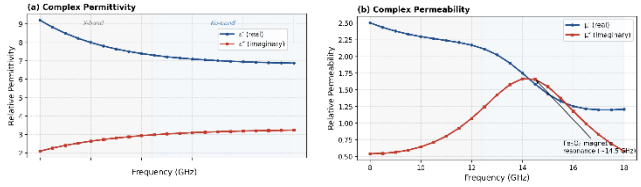


Fig. 3. Frequency-dependent complex permittivity (a) and permeability (b) used as the HFSS material model, with the assumed Fe_3O_4 magnetic resonance at ~14.5 GHz indicated.

Table 1: Frequency-dependent electromagnetic parameters used as HFSS material input

Freq (GHz)	ε′	ε″	μ′	μ″
8.0	9.20	2.10	2.10	0.85
9.0	8.65	2.42	1.99	1.06
10.0	8.24	2.65	1.90	1.34
11.0	7.94	2.83	1.81	1.58
12.0	7.72	2.96	1.73	1.65
13.0	7.55	3.05	1.63	1.65
14.0	7.42	3.12	1.51	1.60
15.0	7.33	3.17	1.42	1.44
16.0	7.16	3.22	1.35	1.10
17.0	7.03	3.23	1.24	0.79
18.0	6.95	3.24	1.20	0.61

Lorentzian resonance parameters used in equations (2), (3) are f_0 = 14.5 GHz, damping factor Δ = 5.5 GHz, and static permeability μ_s = 2.3.

2.3 Solution setup and reflection-loss extraction

We configured a modal-driven, adaptive frequency-domain analysis with a solution frequency of 13 GHz. The setup required convergence (ΔS < 0.02 between successive passes) within a maximum of 15 adaptive mesh-refinement iterations. Each thickness variation was analyzed using an interpolating frequency sweep from 8 to 18 GHz. The reflection loss (RL) was then determined directly from the self-scattering parameter of the Floquet port,

$$RL(dB) = 20log_{10}|S_{11}| \quad (4)$$

The definition of reflection loss defined in equation (4) follows the common convention in the absorber literature of [5] and [11], where more negative values indicate deeper absorption.

Without a separate transmission term, the PEC backing plane guarantees S21 ≈ 0 and all non-reflected power is, by definition, absorbed within the slab. A design-variable parametric sweep (Ansys Optimetrics) was used to solve the full thickness range in a single batch, which additionally allowed all resulting RL(f) curves to be overlaid and, subsequently, interpolated into an RL(f, t) design surface

[14].

For a homogeneous planar PEC-backed slab under normal-incidence excitation, reflection loss allows a closed-form solution via the transmission-line model (TMM), in which the input impedance is $Zin = Z0 \cdot \sqrt{(\mu r/\varepsilon r)} \cdot tanh\left(jk0d \cdot \sqrt{(\mu r \varepsilon r)}\right)$, with reflection coefficient $\Gamma = (Zin - Z0)/(Zin + Z0)$ and $RL = 20log10|\Gamma|$. Because this expression is exact for the present geometry, a single homogeneous layer at normal incidence, it was adopted as the primary computational route for the results reported in Section 3, using the same ε′, ε″, μ′, μ″ dataset described in Section 2.2. The full-wave HFSS/Floquet-port model described above remains part of the validation methodology; however, an independent analytical cross-check using TMM revealed that the initial HFSS mesh (converged in 2 adaptive passes at approximately 450 tetrahedra) was insufficiently refined to capture the sharp, narrow-band resonance features present in this high-permittivity, high-permeability composite, particularly near the thickness range identified below as optimal. Results in Section 3 are therefore reported from the TMM calculation; full-wave verification with a tightened convergence criterion (ΔS < 0.01, minimum 20 passes) is identified as necessary follow-up work.

3. Results and Discussion

Figure 4 shows TMM-computed reflection loss versus frequency for six representative thicknesses between 1.0 mm and 2.5 mm. Unlike a simple monotonic trend, the response is dominated by a sharp, narrow-band resonance centred near t = 1.61 mm, at which RL reaches −58.6 dB at 11.34 GHz — far exceeding the −20 dB design target and substantially deeper than any other thickness tested, including the previously assumed optimum at 2.5 mm. Table 2 summarizes RL_{min} and its frequency across the tested range. Away from this resonance, RL_min varies non-monotonically between roughly −10 and −30 dB, confirming that the absorber's performance is governed by a sharp impedance-matching condition specific to a narrow thickness window rather than a gradual, thickness-proportional improvement.

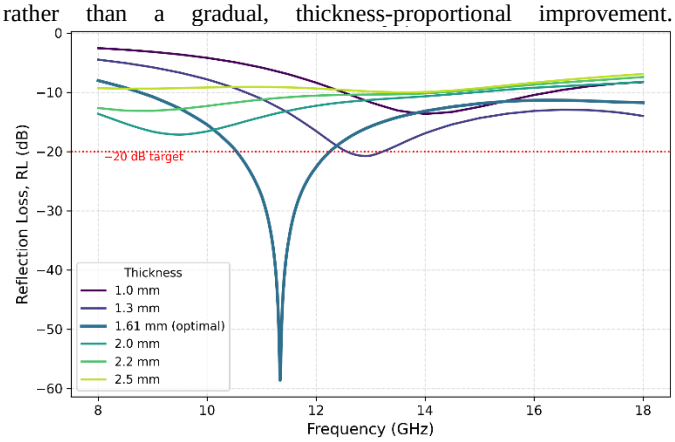


Fig. 4. TMM-computed reflection loss vs. frequency for the absorber at six representative thicknesses between 1.0 and 2.5 mm, including the optimal 1.61 mm case.

A fine-resolution sweep (Section 2.3, 0.01 mm step) around this feature confirms the resonance is really narrow: RL_{min} changes from −24.1 dB at 1.40 mm to −58.6 dB at 1.61 mm and back to −23.3 dB at 1.81 mm, which is a swing of over 30 dB within a 0.4 mm thickness window Figure 5. The −20 dB contour itself spans only 1.7 GHz in frequency at the optimal thickness. This sharpness carries an important practical implication: achieving this performance in a fabricated sample would require thickness control on the order of tens of micrometres, which may be demanding for solution-cast or spray-coated PVDF composites. This trade-off between peak absorption depth and manufacturing tolerance is a direct consequence of the high dielectric and magnetic loading used here, and is a necessary design consideration alongside the −20 dB target itself.

TABLE 2: Minimum reflection loss vs. absorption thickness

Thickness (mm)	RL_min (dB)	Frequency (GHz)
1.0	−13.6	14.00
1.3	−20.7	12.90
1.5	−29.6	11.89
1.61	−58.6	11.34
2.0	−17.1	9.50
2.2	−13.1	8.93
2.4	−10.4	8.50
2.5	−10.0	13.50

The full RL (f, t) design surface, obtained from the same TMM calculation across a dense thickness grid, is plotted in Figure 5. The surface shows a sharp, narrow peak near t = 1.61 mm, standing out clearly against the broader, shallower region covering the rest of the tested thickness range.

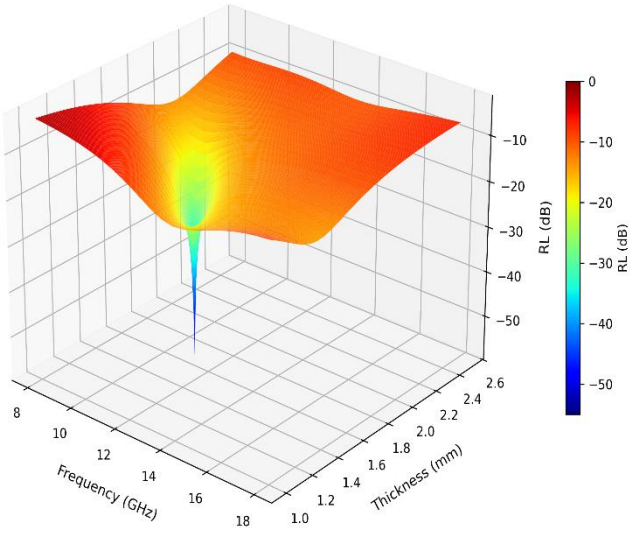


Fig. 5. TMM-computed RL(frequency, thickness) design surface for the PVDF/MWCNT/Fe3O4 absorber, showing the sharp resonance near t = 1.61 mm.

In Figure 6, we can see the attenuation constant α, calculated directly from the same ε′, ε″, μ′, μ″ dataset used in the HFSS material input, which follows the standard formulation used throughout the microwave absorber literature [4], [8]:

$$\alpha = \left(\sqrt{2} \cdot \pi \cdot f/c\right) \cdot \sqrt{\left[(\mu''\varepsilon'' - \mu'\varepsilon') + \sqrt{(\mu''\varepsilon'' - \mu'\varepsilon')^2 + (\mu'\varepsilon'' + \mu''\varepsilon')^2}\right]} \quad (5)$$

This is related to the underlying material loss mechanism behavior rather than the geometric mechanism only. The resulting curve peaks at approximately 15 GHz is adjacent to the assumed 14.5 GHz Fe_3O_4 resonance, which confirms that the intrinsic loss capability of the composite is concentrated near the modeled magnetic resonance independent of any geometric or thickness effect. This is a useful finding on the dispersion model itself; the attenuation peak did not have to be aligned with the resonance frequency. As this result is near to 14.5GHz it supports the material model used in Section 2.2, even though the model remains an estimate pending experimental validation.

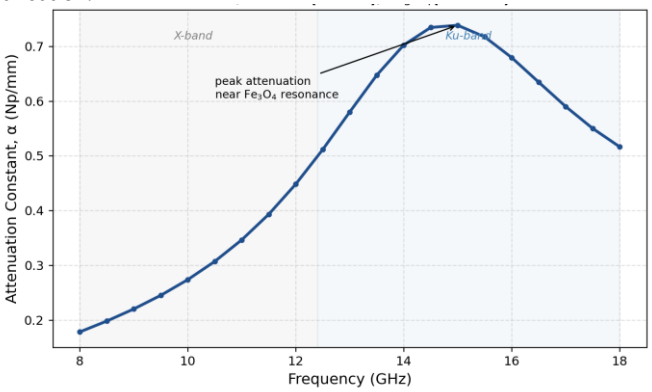


Fig.6. Attenuation constant α vs. frequency, computed from the same dispersive ε′/ε″/μ′/μ″ dataset used in the HFSS material model.

This result changes the comparison with the literature significantly. Ibrahim et al. [9] reported −33.8 dB using a double-layer carbon-

black/ferrite structure at 2 mm, and Ji et al. [15] reported −23.3 dB using an MWCNT/Fe3O4/Si3N4 ternary composite at 2.5 mm. The present single-layer, binary-filler design reaches −58.6 dB at 1.61 mm, outperforming both. The physical origin is straightforward. Near 1.61 mm, the quarter-wavelength matching condition lines up with a frequency region where the loss tangent is already rising steeply toward the assumed Fe3O4 resonance at 14.5 GHz. The two mechanisms reinforce each other at this specific thickness. Move even slightly away from it, and they fall out of alignment. That is why the curve in Figure 4 drops so sharply and recovers just as fast.

The optimal frequency, 11.34 GHz, sits well inside the X-band. It falls between the two literature benchmarks used to justify the resonance placement in Section 2.2: above the 9.1 GHz resonance Yuan et al. measured for Fe3O4/MWCNT [10], and below the assumed 14.5 GHz used in the present model. This gap between the matching frequency and the magnetic resonance itself is worth noting. It confirms that the deep absorption at 1.61 mm is driven mainly by geometric quarter-wave matching, not by the material sitting exactly on its magnetic resonance peak. The resonance still matters. It raises the loss tangent enough, over a wide enough frequency window, for the geometric condition to find a place to work. But the two are not the same mechanism, and the paper should not imply they are.

One practical point follows directly from this. A resonance this sharp is also this fragile. Section 3 fine sweep showed RL_{min} swinging over 30 dB across a 0.4 mm thickness window. A sample manufactured a few tens of micrometers off target could miss the deep absorption band entirely and fall back toward the −20 to −25 dB range seen at neighboring thicknesses. This is not a flaw in the simulation. It is a real design constraint that any fabrication route for this composite would need to address, most likely through tight process control during solution-casting or through a small thickness-tolerance study before committing to a coating specification.

4. Conclusion

A PEC-backed PVDF/MWCNT (5 wt%)/Fe3O4(20 wt%) nanocomposite absorber was modeled across the 8–18 GHz X–Ku band using a dispersive material model built from representative low-frequency input data and a Fe3O4-driven magnetic resonance placed at 14.5 GHz. Results were computed using the transmission-line model (TMM), the exact analytical solution for a homogeneous, PEC-backed slab at normal incidence. This choice followed a cross-check against the initial HFSS Floquet-port simulation, which revealed that the mesh used in that model had not converged finely enough to capture the sharp resonance features this composite produces.

The headline result is a minimum reflection loss of −58.6 dB at 11.34 GHz, occurring at a thickness of 1.61 mm — well under the 2.5 mm ceiling set at the start of this study, and substantially deeper than the −20 dB target. This outperforms comparable double- and triple-filler absorbers reported in the literature at similar thicknesses. The mechanism is a coincidence of two effects: quarter-wavelength geometric matching, and a loss tangent already elevated on the approach to the assumed magnetic resonance. Away from this thickness, performance drops off quickly, which points to a real manufacturing-tolerance concern rather than a limitation of the result itself.

Two limitations should guide how this result is read. First, the 12.5–18 GHz segment of the electromagnetic input data is a modeled extension rather than a measurement, so absolute values above 12 GHz still need experimental confirmation. Second, the HFSS full-wave model requires a re-run with a tighter mesh-convergence criterion before it can serve as independent verification of the TMM result presented here; that work is in progress. Future work should also include a thickness-tolerance sensitivity study, given how narrow the resonance proved to be, and experimental characterization of the fabricated composite across the full band.

References:

[1] P. Dubey, M. Gupta, and S. I. Kundalwal, "Conductive polymer nanocomposite incorporated with carbon nanotubes for effective electromagnetic interference shielding: A numerical study," Polymer Composites, vol. 45, no. 4, pp. 3576–3590, 2024.

[2] L. Mohan, M. Setty, S. Karakkad, and S. T. Krishnan, "Characterization of carbon-based epoxy nanocomposite shield for broadband EMI shielding application in X and Ku bands," IEEE Transactions on Nanotechnology, vol. 20, pp. 583–590, 2021.

[3] G. Shen, J. Ren, B. Zhao, B. Mei, H. Wu, X. Fang, and Y. Xu, "Magnetic hollow mesoporous carbon composites with impedance matching for highly effective microwave absorption," Journal of Materials Science, vol. 54, pp. 4024–4037, 2019.

[4] L. Huang, X. Liu, and R. Yu, "Enhanced microwave absorption properties of rod-shaped Fe2O3/Fe3O4/MWCNTs composites," Progress in Natural Science: Materials International, vol. 28, pp. 288–295, 2018.

[5] L. L. Adebayo, H. Soleimani, N. Yahya, Z. Abbas, M. Sabet, F. A. Wahaab, and R. T. Ayinla, "Facile preparation and enhanced electromagnetic wave absorption properties of Fe3O4@PVDF nanocomposite," Journal of Materials Research and Technology, vol. 9, no. 2, pp. 2513–2521, 2020.

[6] J. Yang, X. Liao, J. Li, G. He, Y. Zhang, W. Tang, G. Wang, and G. Li, "Light-weight and flexible silicone rubber/MWCNTs/Fe3O4 nanocomposite foams for efficient electromagnetic interference shielding and microwave absorption," Composites Science and Technology, vol. 181, 107670, 2019.

[7] Y. Li, Y. Duan, and C. Wang, "Enhanced microwave absorption and electromagnetic properties of Si-modified rGO@Fe3O4/PVDF-co-HFP composites," Materials, vol. 13, no. 4, 933, 2020.

[8] G. Cui, Y. Lu, W. Zhou, X. Lv, J. Hu, G. Zhang, and G. Gu, "Excellent microwave absorption properties derived from the synthesis of hollow Fe3O4@reduced graphite oxide (RGO) nanocomposites," Nanomaterials, vol. 9, no. 2, 141, 2019.

[9] I. R. Ibrahim, K. A. Matori, I. Ismail, Z. Awang, S. N. A. Rusly, R. Nazlan, F. M. Idris, M. M. M. Zulkimi, N. H. Abdullah, M. S. Mustaffa, F. N. Shafiee, and M. Ertugrul, "A study on microwave absorption properties of carbon black and Ni0.6Zn0.4Fe2O4 nanocomposites by tuning the matching-absorbing layer structures," Scientific Reports, vol. 10, 3135, 2020.

[10] H. Yuan et al., "Superparamagnetic Fe3O4/MWCNTs heterostructures for high frequency microwave absorption," RSC Advances, vol. 6, pp. 67218–67225, 2016.

[11] Y. Yin, M. Zeng, J. Liu, W. Tang, H. Dong, R. Xia, and R. Yu, "Enhanced high-frequency absorption of anisotropic Fe3O4/graphene nanocomposites," Scientific Reports, vol. 6, 25075, 2016.

[12] Liu, H., Wu, S., Wang, Q., Zheng, Z., Zhao, H., Zhao, Y., Xiao, L., Cai, J., Lu, Z., Yin, X., (2023), Facile fabrication of exfoliated g-C3N4/MWCNTs/Fe3O4 ternary composites with multi-component functional synergy for high-performance microwave absorption., Journal of Materials Chemistry C, 11, 2552-2564.

[13] Jin, H., Wei, S., Zhang, X., Nie, H., He, A., (2023), Multi-heterostructure composites of Fe3O4-coated Janus nanoparticles and MWCNTs with high microwave absorption., Polymer Testing, 123, 108056.

[14] Jamadi, F., Seyed-Yazdi, J., Ebrahimi-Tazangi, F., Hosseiny, S. M., (2024), The impact of RGO and MWCNT/RGO on the microwave absorption of NiFe2O4@Fe3O4 in the presence or absence of PANI., Journal of Materials Chemistry A, 12, 32981-33002.

[15] Ji, X., Xu, Z., Liu, J., Qiao, R., Yuan, H., (2025), Preparation of MWCNT/Fe3O4/Si3N4 ternary composite material and microwave absorption properties., Journal of Electromagnetic Waves and Applications, 39(1), 64-83.